

resents an imaginary cylinder outlined by the beam cross section (3.5 cm², corresponding to the beam diameter equal to ca. 2.1 cm) and the optical path length of the cell. The absorption volume was then divided, transverse to the beam axis, into cylindrical layers having a base equal to the beam cross section and a thickness of 0.1 cm. When the system is irradiated, SiF₄ molecules absorb energy and E_{abs} values for each layer can be evaluated from (5) and (8). Assuming an instantaneous thermal equilibration in each layer, the maximum temperature was evaluated from (9) within the framework of the standard secant procedure (see e.g. Figures 7 and 8). In the latter estimation the following frequencies (in cm⁻¹) were used:⁹ for SiF₄, 800 (1), 268 (2), 1032 (3), and 389 (3); for H₂, 4397 (1). (The degeneracies of vibrations are indicated parenthetically.) To describe the behavior of the system in time, the chemical changes and shock-wave expansion were considered in 0.5- μ s units. At sufficiently high temperature decomposition of GeH₄ occurs. Thus, if the initial temperature (resulting from the absorption in the layer) is known, the amount of GeH₄ decomposed in the first unit of time can be derived from the standard unimolecular rate equation using k_{uni} values calculated by the RRKM method. (For details see Experimental Section.) Subsequently, the temperature after decomposition in the layer was evaluated on the basis of a relationship analogous to (9), as described earlier. Because the temperature changes only slightly from layer to layer, it can be assumed that expansion takes place only radially from the layer. Considering this effect in the first unit of time the increase of the diameter of a layer was evaluated on the basis of (10). Expansion and rarefaction of the gas brings about an increase in the number of molecules in our imagined extended layer. Thus, the temperature of a layer must decrease. If, again, an assumption of thermal equilibration is made, the temperature of the gas after expansion can be calculated on the basis of energy balances and the right-hand side of (9). This

temperature is the initial one for the determination of the amount of GeH₄ decomposed in the second time unit. Subsequently, the expansion effect was included for the second unit of time as described above. The iterations with respect to time were carried out until the amount of GeH₄ decomposed was less than 0.001 of that actually present in the layer (0.001 level of accuracy; Figure 8). Similar calculations were performed for the remaining layers. If the energy absorbed in the layer is relatively low, the resulting increase of temperature is not high enough to initiate chemical changes. Therefore, the iterations over the layers were stopped when decomposition of GeH₄ in the first time unit was less than 0.001 of that initially present in the layer. The yield of GeH₄ decomposition under given experimental conditions is the sum of contributions from the iterations carried out over all layers and units of time (Figure 9).

To evaluate the dissociation yields, a computer program was developed that took into account all the above-mentioned details and the calculations were performed on an IBM (Model PC XT/AT) personal computer.

To attempt to simplify the problem, we also carried out calculations assuming the same model for the process but using values of rate constants evaluated from the Arrhenius equation. The values of the Arrhenius activation energy and preexponential factor for these calculations were evaluated from the temperature dependence of $k_{\text{uni}}(T, \infty)$ values determined by the RRKM procedure.⁶¹ Unfortunately, decomposition yields thus derived did not fit well to the experimental ones. Similarly, if the time for the completion of reaction is chosen arbitrarily to be 10 μ s, as suggested by some authors,¹⁹⁻²¹ we do not obtain a satisfactory approximation of the experimental results.

Registry No. SiF₄, 7783-61-1; GeH₄, 7782-65-2; Ge, 7440-56-4; H₂, 1333-74-0.

Gas-Phase Reactions of AlO with Small Molecules[†]

J. Mark Parnis,[‡] S. A. Mitchell,* Tanya S. Kanigan, and Peter A. Hackett

Laser Chemistry Group, Division of Chemistry, National Research Council of Canada, 100 Sussex Drive, Ottawa, Ontario, Canada, K1A 0R6 (Received: September 27, 1988; In Final Form: June 14, 1989)

AlO is produced in the gas phase at 296 K by reaction of Al atoms with N₂O following Al atom formation by multiphoton dissociation of trimethylaluminum (TMA). Production and decay of Al and AlO are monitored by laser-induced fluorescence. The combination of efficient vibrational relaxation of AlO by N₂O and low reactivity of AlO with N₂O at room temperature allows studies of AlO reaction kinetics to be carried out with a range of molecules using N₂O as a buffer gas. Second-order rate constants at 296 K (cm³ molecule⁻¹ s⁻¹) are reported for the reactions of ground-state Al(3²P_J) with N₂O, (1.1 ± 0.1) × 10⁻¹¹; ethylene oxide, (1.3 ± 0.1) × 10⁻¹⁰; and TMA, (1.3 ± 0.3) × 10⁻¹⁰ in Ar buffer gas, and for reactions of ground-state AlO(X²Σ⁺, v=0) with ethylene oxide, (2.1 ± 0.5) × 10⁻¹⁰; tetramethylethylene, (1.1 ± 0.4) × 10⁻¹¹; and TMA, (3.0 ± 1.0) × 10⁻¹⁰ in N₂O buffer gas. A third-order rate constant of (4.3 ± 0.4) × 10⁻³² cm⁶ molecule⁻² s⁻¹ is reported for the AlO + CO association reaction in N₂O buffer gas. Reactions of AlO with CO₂ and C₂H₄ showed buffer gas pressure dependent pseudo-second-order rate constants, indicative of processes involving formation of association complexes. Estimates are made of the upper limits for the rate constants for reaction of AlO with N₂O, methane, molecular hydrogen, isobutane, benzene, toluene, CF₃Cl, CF₃Br, and CCl₄, for which the reaction rates at 296 K were negligible.

Introduction

Recently, we have undertaken studies of the reactions of gas-phase Al and Ga atoms with small molecules.¹⁻⁴ We have found the formation of association complexes between these metal atoms and electron-pair donor molecules to be a general aspect of their chemical behavior near room temperature. Such association complexes are of interest in connection with model studies of active sites for adsorption of small molecules on metal surfaces and on

oxide-supported, metal-based catalysts.

In order to pursue this correlation, we have begun to examine other atomic and diatomic models for active sites in catalytic reactions. We report here an investigation of the reactions of a

(1) Parnis, J. M.; Mitchell, S. A.; Rayner, D. M.; Hackett, P. A. *J. Phys. Chem.* **1988**, *92*, 3869.

(2) Mitchell, S. A.; Simard, B.; Rayner, D. M.; Hackett, P. A. *J. Phys. Chem.* **1988**, *92*, 1655.

(3) Mitchell, S. A.; Hackett, P. A.; Rayner, D. M.; Cantin, M. *J. Phys. Chem.* **1986**, *90*, 6148.

(4) Parnis, J. M.; Mitchell, S. A.; Hackett, P. A. *Chem. Phys. Lett.* **1988**, *151*, 485.

[†] Issued as NRCC No. 29469.

[‡] Present address: Department of Chemistry, Trent University, Peterborough, Ontario, Canada K9J 7B8.

diatomic metal oxide, AlO. This molecule was chosen due to its similarity to solid-state O⁻ centers and Li⁺O⁻, which have been implicated in processes involving oxidative coupling of methane on oxide surfaces.⁵ The AlO-H bond enthalpy at 298 K is 111 ± 5 kcal mol⁻¹,⁶ which indicates that hydrogen atom abstraction reactions of AlO with most alkanes, alkenes, and arenes are exothermic. Similarly, the bond enthalpies of OAl-O (96 ± 10 kcal mol⁻¹) and OAl-Cl (128 ± 7 kcal mol⁻¹)⁶ suggest that O atom and halogen atom abstraction reactions are also possible. As AlO is a highly ionic molecule with a calculated dipole moment of 4–5 D,^{7,8} dipole-dipole and dipole-induced dipole forces are expected to contribute significantly to attractive interactions between AlO and small polar or polarizable molecules.

The chemistry of diatomic metal oxides is relatively unknown. This is due in part to the difficulty involved in producing metal oxides in a convenient form for chemical studies. We have successfully used multiphoton dissociation of organometallic precursors as a source of metal atoms at room temperature.⁹ This technique has allowed spectroscopic and kinetic studies to be done with metallic elements which are not conveniently vaporized by using thermal sources. In the present work we have coupled the MPD of trimethylaluminum with a rapid Al atom oxidation reaction to allow studies of reaction kinetics of a refractory metal oxide, AlO. Such an approach is potentially of general utility for studies of the reaction kinetics of other metal-containing diatomic species.

Aluminum atom oxidation reactions with several molecules have previously been reported. Diatomic AlO chemiluminescence has been observed by Rosenwaks et al.¹⁰ following Al atom reactions with N₂O, O₂, O₃, and other oxidants. Intense A²Π → X²Σ⁺ and weaker B²Σ⁺ → X²Σ⁺ AlO emission was observed with both O₃ and N₂O. Gole et al.^{11–13} have reported a detailed analysis of the chemiluminescence produced in these reactions. An electron-jump model¹⁴ has been suggested for the reaction of Al atoms with O₃,^{11,15} while the Al + N₂O reaction is believed to proceed by a more complex mechanism.¹¹ Detailed reaction dynamics studies of the Al + O₂ reaction have been done by Dagdigian et al.^{16,17} in a beam-gas configuration. Recently, Costes et al.¹⁸ have examined the dependence of AlO product rotational and vibrational state distributions on the collision energy of Al atoms with O₂, CO₂, and SO₂ in crossed supersonic molecular beams.

Previous work on metal oxide kinetics has been reported by Fontijn and co-workers,^{19–22} who have used high-temperature, fast-flow reactors to study several group 13 metal oxide oxidation reactions. The reactions of AlO with O₂ and SO₂^{19,20} both show rate constants that are lower than those of the corresponding metal atom oxidation reactions, such that sequential oxidation reaction kinetics studies could be carried out. The AlO + CO₂²¹ and BO + O₂²² reactions have also been studied in flow systems, the former

showing a slightly negative activation energy which has been interpreted as arising from an intermediate AlO-CO₂ complex which preferentially dissociates to reactants.

Several reactions of NaO with small molecules have been studied in connection with interest in the atmospheric chemistry of Na.²³ Howard et al.^{24,25} have recently reported gas-phase kinetic studies of NaO reactions with O₃, N₂O, H₂, and H₂O. Reactions of NaO with HCl, CO, and H atoms are also known.^{26–28} The highly ionic nature of NaO results in a varied chemistry in which loss of O to yield Na atoms as well as O atom and H atom abstraction are found. Dipole-dipole and dipole-induced dipole interactions play a significant role in these processes, some of which have been suggested to occur via an electron-jump mechanism.²⁴

We report here results from studies of the reactions of ground-state AlO(X²Σ⁺, v=0) with several small molecules. The tendency for AlO to form association complexes with electron-pair donor molecules is evident, as is the absence of a significant abstraction reaction chemistry at room temperature. Results for oxidation reactions of Al atoms with N₂O and ethylene oxide, two oxidants chosen as oxygen atom donors for production of AlO, are also reported. The reaction of Al atoms with N₂O is about 81 kcal mol⁻¹ exothermic, based upon D^o₀(AlO) = 121.3 kcal mol⁻¹¹⁸ and D^o₀(NN-O) of 40 kcal mol⁻¹.⁶ This reaction was found to be convenient as a source of AlO for reaction kinetics studies, since AlO shows no measurable reactivity with N₂O at room temperature. Thus, N₂O could be used as a buffer gas for the AlO reaction kinetics studies reported here.

Experimental Section

The experimental arrangement for laser-photolysis, laser-fluorescence studies of Al and Ga atom reaction kinetics has been described previously.^{1–3} In view of the novelty of the present approach for kinetic studies of metal oxide diatomic molecules, and as a number of changes have been made to the apparatus, a detailed description of the experiment is given here.

Production and Monitoring of Al Atoms. Al atoms were produced by visible multiphoton dissociation (MPD) of trimethylaluminum (TMA) in a static-pressure gas cell,²⁹ using the focused output of a pulsed dye laser (photolysis laser). Ground-state Al atoms were detected by saturated resonance fluorescence excitation at 394.40 nm (4²S ← 3²P_{1/2}), using a second, independently triggered, pulsed dye laser (probe laser). The time delay between the photolysis and probe laser pulses was scanned in order to monitor the time dependence of the population of ground-state Al atoms following the photolysis pulse. The interpulse delay was scanned in preset increments and the laser-induced fluorescence signal from 50–100 shots averaged at each setting. The entire delay range was swept 4–6 times to allow monitoring of the sample stability during the data acquisition period. With the laser repetition rate at 20 Hz, and averaging 60 shots at each of 100 successive delay increments, each kinetic trace took 5 min to record.

The photolysis and probe dye lasers were both Lumonics Model EPD-330, pumped by separate Lumonics XeCl excimer lasers. An amplifier was used in the photolysis dye laser, which produced pulses of 1–4 mJ at 440 nm, whereas only the oscillator was used in the probe dye laser, which produced pulses of ≈ 300 μJ at 394.4

(5) Lin, C.-H.; Ito, T.; Wang, J.-X.; Lunsford, J. H. *J. Am. Chem. Soc.* **1987**, *109*, 4808. Mehandru, S. P.; Anderson, A. B.; Bradzil, J. F. *J. Am. Chem. Soc.* **1988**, *110*, 1715 and references cited therein.

(6) *JANAF Thermochemical Tables*, 3rd ed.; Dow Chemical Co.: Midland, MI; *J. Phys. Chem. Ref. Data* **1985**, *14*, Suppl. No. 1.

(7) Yoshimine, M.; McLean, A. D.; Liu, B. *J. Chem. Phys.* **1973**, *58*, 4412.

(8) Lengsfeld, B. H.; Liu, B. *J. Chem. Phys.* **1982**, *77*, 6083.

(9) Mitchell, S. A.; Hackett, P. A. *J. Chem. Phys.* **1983**, *79*, 4815.

(10) Rosenwaks, S.; Steele, R. E.; Broida, H. P. *J. Chem. Phys.* **1975**, *63*, 1963.

(11) Lindsay, D. M.; Gole, J. L. *J. Chem. Phys.* **1977**, *66*, 3886.

(12) Sayers, M. J.; Gole, J. L. *J. Chem. Phys.* **1977**, *67*, 5442.

(13) Gole, J. L.; Zare, R. N. *J. Chem. Phys.* **1972**, *57*, 5331.

(14) Herschbach, D. R. *Adv. Chem. Phys.* **1966**, *10*, 319.

(15) Kolb, C. E.; Gersh, M. E.; Herschbach, D. R. *Combust. Flame* **1975**, *25*, 31.

(16) Dagdigian, P. J.; Cruse, H. W.; Zare, R. N. *J. Chem. Phys.* **1975**, *62*, 1824.

(17) Pasternack, L.; Dagdigian, P. J. *J. Chem. Phys.* **1977**, *67*, 3854.

(18) Costes, M.; Naulin, C.; Dorthe, G.; Vauchamps, C.; Nouchi, G. *Faraday Discuss. Chem. Soc.* **1987**, *84*, 75.

(19) Felder, W.; Fontijn, A. *J. Chem. Phys.* **1976**, *64*, 1977.

(20) Fontijn, A.; Felder, W. *J. Chem. Phys.* **1979**, *71*, 4854.

(21) Rogowski, D. F.; English, A. J.; Fontijn, A. *J. Phys. Chem.* **1986**, *90*, 1688.

(22) Llewellyn, I. P.; Fontijn, A.; Clyne, M. A. *Chem. Phys. Lett.* **1981**, *84*, 504.

(23) Chapman, S. *Astrophys. J.* **1939**, *90*, 309. Ferguson, E. E. *Geophys. Res. Lett.* **1978**, *5*, 1035.

(24) Ager, J. W., III; Talcott, C. L.; Howard, C. J. *J. Chem. Phys.* **1986**, *85*, 5584.

(25) Ager, J. W., III; Howard, C. J. *J. Chem. Phys.* **1987**, *87*, 921.

(26) Silver, J. A.; Stanton, A. C.; Zahniser, M. S.; Kolb, C. E. *J. Phys. Chem.* **1984**, *88*, 3123.

(27) Benson, R. C.; Barger, C. B.; Walker, R. E. *Chem. Phys. Lett.* **1975**, *35*, 161.

(28) Fenimore, C. P.; Kelso, J. R. *J. Am. Chem. Soc.* **1950**, *72*, 5045.

(29) Triethylaluminum (TEA) was also used as a source of Al atoms in order to test for source-dependent effects on Al atom reaction kinetics. Using TEA, a rate constant for the Al + N₂O reaction was obtained at 298 K which was the same as that obtained for this reaction by using TMA as an Al atom source, within experimental error. Thus, both TMA and TEA are useful sources of gas-phase Al atoms via the visible multiphoton dissociation process.

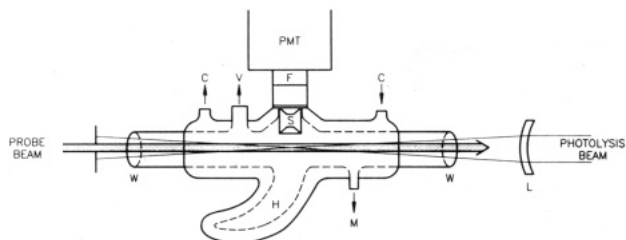


Figure 1. Illustration of double-walled glass cell for gas-phase metal atom and metal oxide reaction kinetics. Ray diagrams indicate the photolysis and detection laser beam geometries. Probe beam diameter has been exaggerated for clarity. The symbols have the following meanings: W, angled windows; V, port to evacuation pump; M, port to all-metal vacuum line; C, coolant inlet and outlets; H, glass horn; S, double aperture assembly; F, filter(s); PMT, photomultiplier tube and housing; L, photolysis laser focusing lens.

nm. Pulse durations were ≈ 10 ns. The beams were aligned collinear and counterpropagating through the center of the reaction cell, using lenses to collimate (≈ 1 cm beam diameter) and then focus the photolysis beam (focal length 25 cm), and a series of lenses, attenuators, and apertures to produce a collimated probe beam ≈ 1 mm in diameter and with a pulse energy of ≈ 100 nJ. The focal region of the photolysis beam was in the fluorescence viewing zone at the center of the cell.

Laser-induced fluorescence (LIF) from Al atoms (396.15, 394.40 nm) was viewed by a Hamamatsu 1P28 photomultiplier tube (PMT) through a band-pass filter (Corning 7-51), which blocked the scattered 440-nm photolysis light. Output pulses from the PMT were amplified by a Keithly Model 427 current amplifier (10^6 or 10^7 V/A gain) to produce voltage pulses which were typically several volts in amplitude and which had a rise time of 30 μ s. The peak amplitudes were read by a NRC-built sample-and-hold circuit and transferred to a Hewlett-Packard 3437A system voltmeter, where they were digitized and passed via the IEEE 428 GPIB to a Tektronix 4052 microcomputer for display, storage, and subsequent analysis. The microcomputer also controlled the timing between the photolysis and probe laser pulses, through a Berkeley Nucleonics Corporation Model 7030 programmable delay generator.

Reaction Cell. The reaction cell, illustrated in Figure 1, was a double-walled, 30 cm long, 2 cm internal diameter Pyrex tube fitted with angled end windows (W) for passing the laser beams, a side window for viewing fluorescence, and gas inlet and outlet ports for connection to an all-metal, high-vacuum line on the inlet side (M) and a 4-in. diffusion pump on the outlet side (V). The angled end windows (Suprasil quartz) were glued with Varian Torr-Seal to short lengths of Pyrex tubing and fastened to the cell by means of Ultratorr vacuum fittings. Fluorescence was observed through a pair of 5 mm diameter apertures placed in the side arm of the cell (S), opposite the Wood's horn (H). The double-walled construction of the cell allowed circulation of temperature-controlled ethylene glycol (C). Temperature measurement was by a chromel-alumel thermocouple probe positioned near the fluorescence viewing zone. Pressure measurement was by Baratron capacitance manometers.

In order to produce stable pressures of TMA in the desired range (10–50 mTorr), and stable LIF signals for Al atoms, it was necessary to condition the cell and vacuum line extensively with relatively high pressures of TMA (≈ 5 Torr). After this treatment the Al atom LIF signal was stable to within $\approx 10\%$ for at least 30 min.

Production and Monitoring of AlO. For studies of AlO kinetics, Al atoms were converted quantitatively to AlO by reaction in a large excess of N_2O (200–750 Torr). Ground-state AlO ($X^2\Sigma^+, v=0$) was detected by saturated LIF with excitation at 464.8 nm ($B(v=1) \leftarrow X(v=0)$) and observation of $B(v=1) \rightarrow X(v=2)$ emission at 507.9 nm.³⁰ An interference filter (centered at 510 nm with a 10-nm band-pass) was used in combination with a low

fluorescence cutoff filter (transmission at $\lambda > 500$ nm) to block scattered light from the photolysis laser and background emission from chemiluminescence (see below). Vibrationally excited AlO ($X^2\Sigma^+, v=1,2$) was detected by $B \leftarrow X$ excitation at 467.2 nm (2,1) and 469.5 nm (3,2), with observation of emission at 510.2 nm (2,3) and 512.3 nm (3,4), respectively.³⁰ The time dependence of the AlO ($X^2\Sigma^+, v=0,1,2$) population was observed as described above for Al, except that 300–500 pulses were averaged at each delay setting to improve the signal-to-noise ratio.

Chemiluminescence from the reaction of Al with N_2O ^{10,11} appeared as a noisy background to the LIF signal. In addition, scattered photolysis laser light (440 nm) excited fluorescence from various components of the reaction cell, including the Torr-Seal epoxy that was used to attach the end windows. This fluorescence had a component which fell within the band-pass of our interference filter and therefore contributed to the background. The total background signal was similar in magnitude to the AlO LIF signal. The time dependence of the background emission was observed by coupling the output of the PMT through 50 Ω to a Tektronix Model 7D20 programmable digitizer.

Interpretation of Kinetic Data. Reactions of Al and AlO were carried out under pseudo-first-order conditions, where the pressure of the reactant greatly exceeded the pressure of Al or AlO. Second-order rate constants (pseudo second order in the case of termolecular reactions) were therefore obtained from the slopes of plots of the pseudo-first-order removal rate for Al or AlO against the pressure of the reactants.

A limiting feature of our experimental approach, involving visible MPD of TMA for production of free Al atoms, arises from the occurrence of rapid reactions of both Al and AlO with the precursor molecule TMA. The mechanisms of these removal processes involving TMA are not known in detail but likely involve the formation of association complexes.³¹ The occurrence of these reactions at near-gas-kinetic rates has the effect of constraining the useful pressure range of TMA to ≈ 10 –50 mTorr. The pseudo-first-order removal rate in the absence of an added reactant is therefore non-zero and leads to a positive intercept in plots used to measure the second-order and pseudo-second-order rate constants. From experience with metal carbonyl compounds such as $Cr(CO)_6$,³² for which reaction of the free metal atom with the precursor molecule does *not* occur, we have found that diffusion of the metal atom out of the probe laser detection zone occurs on a much longer time scale than that considered here. Diffusion therefore does not contribute to the observed removal rate of Al or AlO.

Production of Al atoms is confined to the focal region of the photolysis laser beam at the center of the cell. The focal region is estimated to be 50–100 μ m in diameter and 2–5 mm in length. This arrangement has the advantage that the windows of the cell which pass the photolysis laser beam remain free of deposits from dissociated TMA. As the time scale for the reactions investigated is very much shorter than that for diffusion across the width of the cell, wall reactions cannot contribute to the observed removal processes, and need not be considered.

The straightforward analysis of our kinetic data according to standard methods entails several assumptions, which we now consider. It is assumed that the LIF signal is linear with respect to the number of Al atoms or AlO molecules in the probe laser beam. This was ensured in our experiments by saturating the excitation process, so that the *fraction* of atoms or molecules excited by the laser was maximized and was independent of the number of absorbing species present. For practical purposes,

(31) The fate of the methyl radicals produced following MPD of TMA is not known. Contributions to Al atom loss due to reaction with methyl radicals are believed to be insignificant, since the exponential form of the Al atom decay in the absence of quenchers other than TMA is not compatible with a reaction of Al atoms with a very localized, low concentration of methyl radicals. Such a reaction would exhibit highly nonexponential decay behavior due to departures from pseudo-first-order conditions and rapidly changing methyl radical and aluminum atom concentrations arising from diffusion of these species from the photolysis laser focal region.

(32) Parnis, J. M.; Mitchell, S. A.; Hackett, P. A. 1988, unpublished results from work in progress.

(30) Gatterer, A.; Junkes, J.; Salpeter, E. W. *Molecular Spectra of Metallic Oxides*; Specola Vaticana: Citta del Vaticano, 1957.

saturation is attained when the LIF signal no longer increases with increased excitation pulse energy.

It is a basic requirement of the mode of data acquisition employed that the gas mixture in the focal region of the photolysis laser beam be completely renewed by diffusion from the bulk gas between successive laser shots. This was verified by the observation of a stable Al or AlO LIF signal (at arbitrary interpulse delay intervals) over many thousands of shots. Incomplete renewal of the sample mixture between shots would have resulted in a drastic loss of signal, at a rate dependent upon the laser repetition rate. We estimate that the time required for complete sample recovery is less than 1 ms, which compares with 50 ms as the interval between laser shots. Rapid recovery of the sample is ensured by the small volume of the photolysis focal region. Stability of the LIF signal also demonstrates that the sample mixture is stable with respect to decomposition of TMA in the bulk gas or on the cell walls (resulting for example from air leaks or impurities in the reactant gases). This was monitored continuously by repeatedly sweeping the interpulse delay over the full delay range during data collection.

It is assumed that the addition of reactant gases has no effect on the rate of removal of Al or AlO by TMA. This seems justifiable but is difficult to verify. Clearly, the potential for problems arising from this is greater when the removal rate by TMA remains a significant fraction of the total removal rate over the full range of pressures of the added reactant. In all cases, the pressure of the reactant was much lower than that of the buffer gas, so that effects due to changes in the total pressure did not arise.

It is further assumed that the added reactant gases (apart from TMA) are transparent to both the photolysis and probe laser pulses, so that reactions involving laser-heated reactants or reactant photolysis products need not be considered. Although the focused photolysis laser beam deposits energy into the gas by fragmentation of TMA molecules, the amount deposited is small, and thermalization of the reactants is rapid. This is shown, for example, by the rapid equilibration of Al atoms between the $^2P_{3/2}$ and $^2P_{1/2}$ fine-structure levels in Ar buffer gas.² The small size of the focal region of the photolysis laser beam, the low pressure of TMA, and the high pressure of buffer gas used in our experiments are significant factors in this connection. We have carried out photoacoustic measurements which indicate that most of the reactant molecules considered in this study are transparent to the photolysis laser pulse, exhibiting no tendency for significant multiphoton absorption at 440 nm under the conditions used in our experiments. Only for benzene and tetramethylethylene were photoacoustic signals observed. For these and several other reactants, including ethylene oxide and TMA, we investigated the dependence of the Al atom removal rate on the photolysis laser pulse energy in the range 1–4 mJ. In no case was a significant effect observed. Thus, there is no indication that significant photolysis or heating of any of the reactants occurred.

In the case of reactions involving AlO, it is assumed that all of the AlO molecules undergo rapid equilibration following their formation by the reaction of Al atoms with N_2O . This assumption is discussed below.

Reactants. Electronic grade trimethylaluminum was supplied by Alfa Products. Research purity argon, hydrogen, methane, carbon dioxide, and carbon monoxide as well as CP grade ethylene oxide, deuterium, and ethylene, instrument grade isobutane, and >99% chlorotrifluoromethane were supplied by Matheson of Canada. Grade 4.5 nitrous oxide (>99.995%) was supplied by Airco. Bromotrifluoromethane was supplied by SCM Chemicals. Spectrophotometric grade liquids were supplied by Aldrich (2,3-dimethylbut-2-ene, benzene, and carbon tetrachloride) and BDH (toluene). Whenever possible, reactants were extensively degassed by freeze-pump-thaw cycling before use.

Results

Al Atom Oxidation by N_2O and C_2H_4O . The reactions of ground-state Al($3s^23p^1, ^2P_J$) atoms with N_2O and ethylene oxide (C_2H_4O) were examined as sources of AlO for kinetics studies. Typical raw data illustrating removal of Al atoms under pseu-

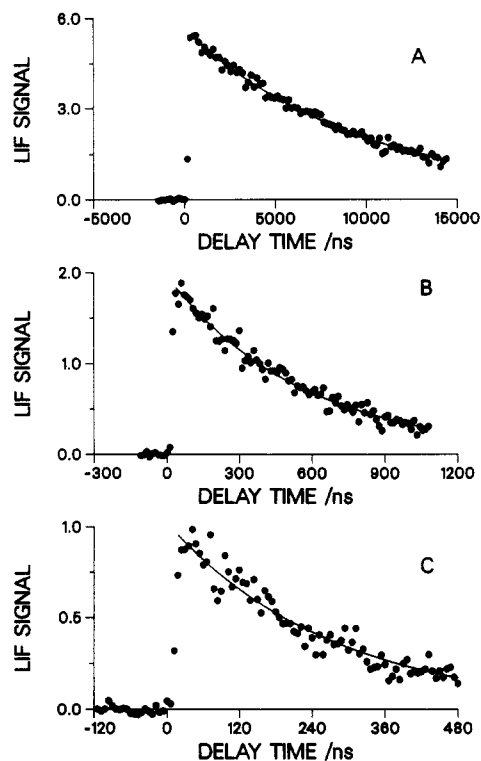


Figure 2. Decay data showing the variation in the Al atom LIF signal with delay time between photolysis and probe laser pulses for (A) 20 mTorr of TMA in 300 Torr of Ar buffer gas, (B) 5 Torr of N_2O and 20 mTorr of TMA in 300 Torr of Ar buffer gas, and (C) 10 Torr of N_2O and 20 mTorr of TMA in 300 Torr of Ar buffer gas. Solid curves represent the best fit to a simple exponential decay expression.

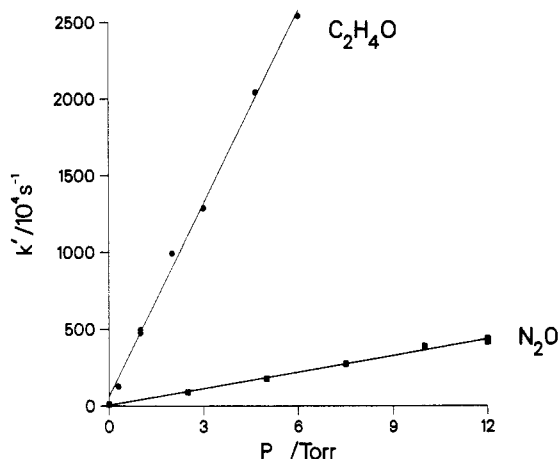


Figure 3. Graph of the variation in the pseudo-first-order rate constant for removal of Al atoms ($^2P_{1/2}$) by ethylene oxide (upper trace) and N_2O (lower trace) at 296 K. Argon buffer gas pressure used was 200 Torr (C_2H_4O) and 300 Torr (N_2O).

do-first-order conditions at various pressures of N_2O are shown in Figure 2. Figure 3 illustrates the variation of the pseudo-first-order rate constant, k' , with N_2O and C_2H_4O pressure, respectively. Second-order rate constants of $(1.1 \pm 0.1) \times 10^{-11} \text{ cm}^3 \text{ molecule}^{-1} \text{ s}^{-1}$ (N_2O) and $(1.3 \pm 0.1) \times 10^{-10} \text{ cm}^3 \text{ molecule}^{-1} \text{ s}^{-1}$ (C_2H_4O) were obtained. Both oxidation reactions showed no appreciable dependence of the second-order rate constant on Ar buffer gas pressure between 50–300 Torr (N_2O) and 100–700 Torr (C_2H_4O). Direct observation of AlO was made by LIF in both cases, indicating that AlO is produced in both reactions. In the absence of an added reactant, the observed decay of the Al atoms is due to reaction with the precursor, TMA (Figure 2A), for which a second-order rate constant of $(1.3 \pm 0.3) \times 10^{-10} \text{ cm}^3 \text{ molecule}^{-1} \text{ s}^{-1}$ was obtained.

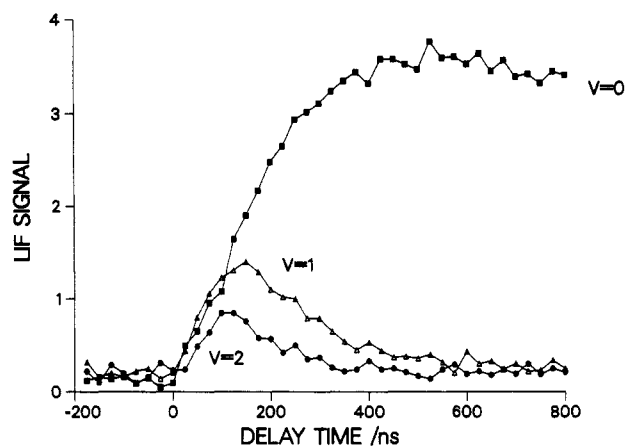


Figure 4. Graph of the variation in $\text{AlO}(X^2\Sigma^+, v=0,1,2)$ LIF signals with delay time between photolysis and probe laser pulses for 500 Torr of N_2O buffer gas pressure at 296 K.

TABLE I: Rate Constants for Reactions of Ground-State $\text{AlO}(X^2\Sigma^+, v=0)$ with Various Molecules at 296 K

reactant	range ^a	rate constant ^{b,c}
Association Reactions		
$\text{C}_2\text{H}_4\text{O}$	0–0.7	$(2.1 \pm 0.5) \times 10^{-10}$
CO	21	$(4.3 \pm 0.4) \times 10^{-32}$ (200–700)
CO_2	0–5	$(1.1\text{--}1.7) \times 10^{-11}$ (200–700)
C_2H_4	0–5	$(1.2\text{--}2.6) \times 10^{-11}$ (200–600)
$\text{C}_2(\text{CH}_3)_4$	0.5–3	$(1.1 \pm 0.4) \times 10^{-11}$
C_6H_6	0–6	$< 5 \times 10^{-13}$
$\text{C}_6\text{H}_5\text{CH}_3$	0–5	$< 5 \times 10^{-13}$
Atom Abstraction Reactions		
N_2O	0–700	$< 1 \times 10^{-15}$
<i>i</i> - C_4H_{10}	0–40	$< 1 \times 10^{-13}$
CH_4	0–50	$< 5 \times 10^{-14}$
H_2	0–50	$< 5 \times 10^{-14}$
CF_3Cl	0–15	$< 5 \times 10^{-14}$
CF_3Br	0–10	$< 5 \times 10^{-14}$
CCl_4	0–5	$< 5 \times 10^{-13}$

^a Pressure range of reactant gas studied, in Torr. ^b All rate constants are in units of $\text{cm}^3 \text{ molecule}^{-1} \text{ s}^{-1}$ except that reported for CO, which is a third-order rate constant in units of $\text{cm}^6 \text{ molecule}^{-2} \text{ s}^{-1}$. ^c Pseudo-second-order rate constants for termolecular are given as a range and are followed by the N_2O buffer gas pressure range (in parentheses, Torr) over which the rate constants were obtained. Other second-order rate constants are for reaction at 500 Torr of N_2O buffer gas pressure.

Production of Ground-State $\text{AlO}(X^2\Sigma^+, v=0)$ in N_2O . The production of ground-state $\text{AlO}(X^2\Sigma^+, v=0)$ as well as vibrationally excited $\text{AlO}(X^2\Sigma^+, v=1,2)$ was monitored by LIF following multiphoton dissociation of TMA in N_2O buffer gas. Figure 4 illustrates the variation in the LIF signal intensity with the photolysis-probe interpulse delay for excitation of AlO at the (B ← X) $\Delta v = +1$ sequence bandhead position³⁰ for $v'' = 0,1,2$ in 500 Torr of N_2O buffer gas. These results indicate that relaxation of electronically and vibrationally excited states of AlO is complete after about 500 ns. The decay of the ground-state $\text{AlO}(X^2\Sigma^+, v=0)$ LIF signal after this point is due to the reaction of AlO with TMA, for which a second-order rate constant of $(3 \pm 1) \times 10^{-10} \text{ cm}^3 \text{ molecule}^{-1} \text{ s}^{-1}$ was measured. No evidence for slow radiative or nonradiative relaxation of metastable excited states of AlO was found in the present study. From data of the type shown in Figure 4, and under the simplifying assumption that each vibrational relaxation process may be considered independently of the others, the rate constants for collisional relaxation of $v=1,2$ of $\text{AlO}(X^2\Sigma^+)$ by N_2O were estimated to be $\sim 5 \times 10^{-13} \text{ cm}^3 \text{ molecule}^{-1} \text{ s}^{-1}$, corresponding to a cross section of about 0.1 \AA^2 . Relaxation rates are somewhat slower at lower pressures of N_2O , such that vibrational relaxation takes about 1500 ns at 200 Torr of N_2O pressure. No evidence was found to suggest that AlO reacts appreciably with N_2O at room temperature.

The reaction of Al with N_2O generates a strong signal due to chemiluminescent relaxation of the AlO B state^{10,11} which is

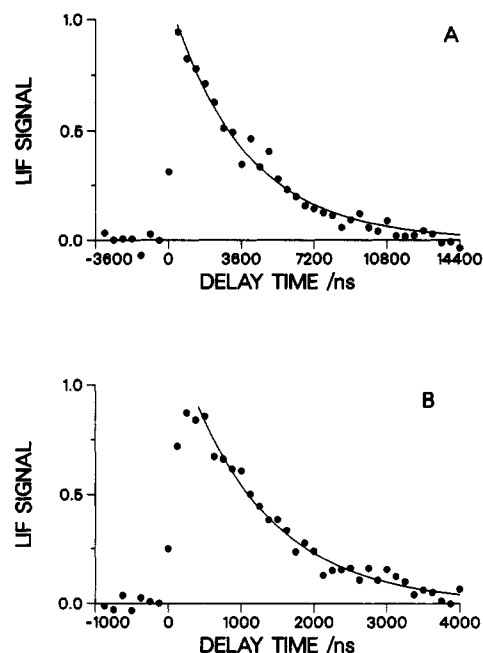


Figure 5. Decay data showing the variation in the $\text{AlO}(X^2\Sigma^+, v=0)$ LIF signal with delay time between photolysis and probe laser pulses for (A) 20 mTorr of TMA in 700 Torr of N_2O buffer gas and (B) 1 Torr of CO_2 and 20 mTorr of TMA in 700 Torr of N_2O buffer gas. Solid curves represent the best fit to a simple exponential decay expression.

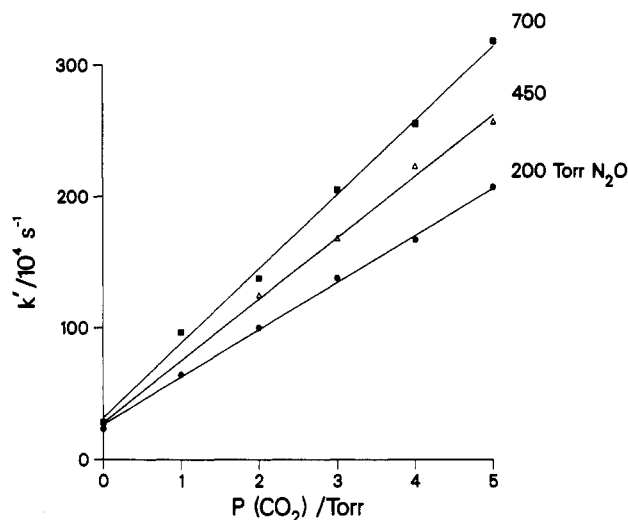


Figure 6. Graph of the variation in the pseudo-first-order rate constant for removal of $\text{AlO}(X^2\Sigma^+, v=0)$ by CO_2 at three pressures of N_2O buffer gas (200, 450, 700 Torr) at 296 K. TMA pressure was 20 mTorr.

independent of the probe laser. Time-resolved studies of this signal showed that the $\text{AlO}(B \rightarrow X)$ chemiluminescence is negligible after about 200 ns for N_2O pressures greater than 400 Torr. This indicates that relaxation of the AlO B state is complete within this time range.

AlO Reactions with Small Molecules. Reactions of ground state $\text{AlO}(X^2\Sigma^+, v=0)$ with a range of small molecules were examined under pseudo-first-order conditions at 296 K in N_2O buffer gas (200–700 Torr). Table I summarizes the results of these studies. Representative decay data for the reaction of AlO with CO_2 are shown in Figure 5. The reactions of AlO with CO_2 , CO, and ethylene exhibit a dependence of the pseudo-second-order rate constant on the buffer gas pressure. This effect is illustrated for CO_2 and ethylene in Figures 6 and 7. The pseudo-second-order rate constants for these reactions were found to vary approximately linearly over the range 200–600 Torr of N_2O buffer gas pressure. However, extrapolation to low pressure yielded a nonzero intercept, indicating that the pressure regime investigated for these termolecular reactions is in an intermediate region between sec-

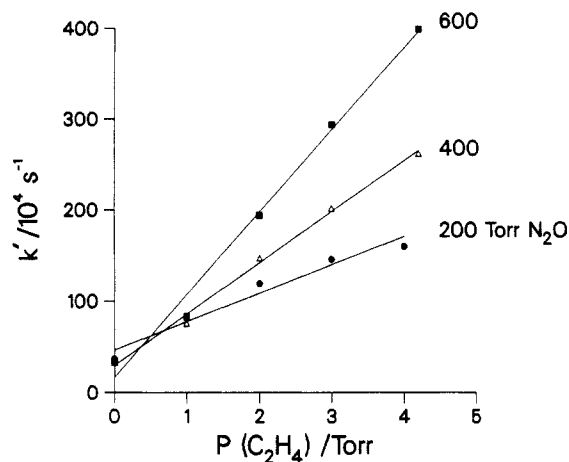


Figure 7. Graph of the variation in the pseudo-first-order rate constant for removal of $\text{AlO}(X^2\Sigma^+, \nu=0)$ by C_2H_4 at three pressures of N_2O buffer gas (200, 400, 600 Torr) at 296 K. TMA pressure was 30 mTorr.

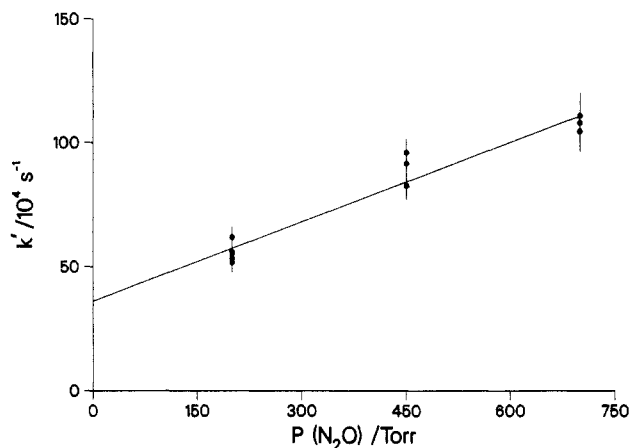


Figure 8. Graph of the variation in the pseudo-first order rate constant for removal of $\text{AlO}(X^2\Sigma^+, \nu=0)$ by 21 Torr of CO with pressure of N_2O buffer gas. TMA pressure was 20 mTorr.

ond-order kinetics at higher pressure and third-order kinetics at low pressure. The low-pressure regime was not accessible in our experiments due to the requirement for N_2O pressures in excess of 200 Torr in order to ensure rapid relaxation of AlO produced in the $\text{Al} + \text{N}_2\text{O}$ reaction. The $\text{AlO} + \text{CO}$ reaction was found to be in the low-pressure (third-order) region over the range 200–750 Torr of N_2O pressure (Figure 8). The third-order rate constant for this reaction with N_2O as a buffer gas is given in Table I. The reactions of AlO with tetramethylethylene (TME) and ethylene oxide ($\text{C}_2\text{H}_4\text{O}$) showed second-order kinetic behavior between 200 and 700 Torr buffer gas pressure. The data for these reactions are plotted in Figures 9 and 10, and the rate constants given in Table I. No reaction between AlO and methane, molecular hydrogen, isobutane, benzene, toluene, CF_3Cl , CF_3Br , and CCl_4 was detectable under these reaction conditions. Estimates of upper limits for rate constants for removal of $\text{AlO}(X^2\Sigma^+, \nu=0)$ by these molecules are given in Table I, which also gives the pressure ranges investigated for all reactants.

Discussion

Preparation of Ground-State AlO for Kinetics Studies. The results given here demonstrate that kinetic studies of reactions of AlO can be done using N_2O as a buffer gas in a static gas cell. The success of this approach results from several aspects of the reactions of Al and AlO with N_2O which allow ground-state $\text{AlO}(X^2\Sigma^+, \nu=0)$ to be formed in good yield following multiphoton dissociation of TMA. These are as follows. (1) Al atoms react with N_2O at 296 K at a rate which is about 1/30 gas kinetic. Thus, conversion of Al to AlO is complete after about 25 ns at 200 Torr of N_2O pressure. (2) Collisional relaxation of vibrationally excited AlO occurs in N_2O such that all AlO is in its

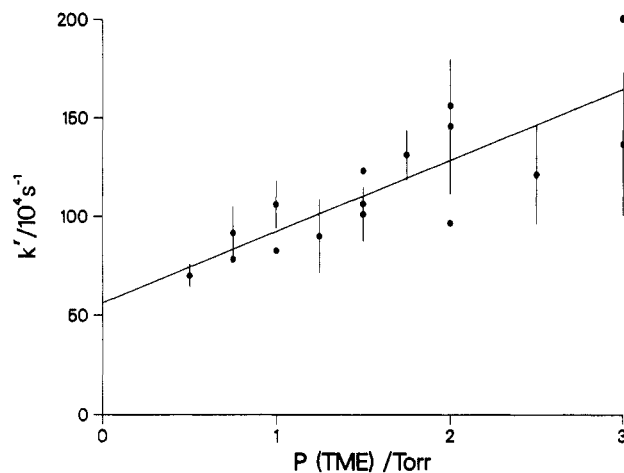


Figure 9. Graph of the variation in the pseudo-first-order rate constant for the removal of $\text{AlO}(X^2\Sigma^+, \nu=0)$ with pressure of tetramethylethylene (TME) at 30 mTorr of TMA and 500 Torr of N_2O buffer gas pressure. The slope yields the second-order rate constant. Some error bars have been omitted for clarity.

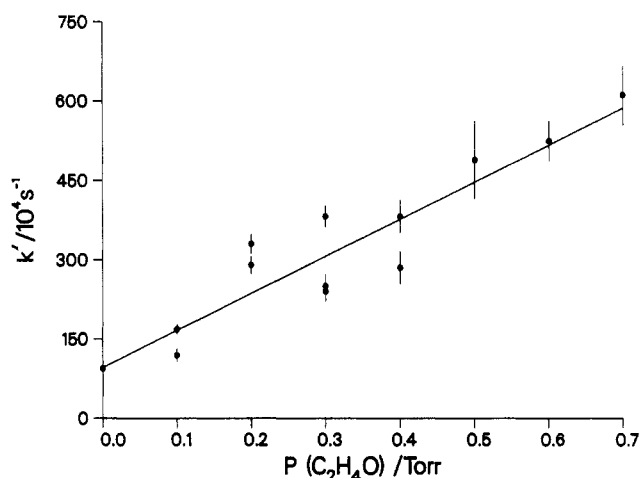


Figure 10. Graph of the variation in the pseudo-first-order rate constant for removal of $\text{AlO}(X^2\Sigma^+, \nu=0)$ with pressure of ethylene oxide at 50 mTorr of TMA and 500 Torr of N_2O buffer gas pressure. The slope yields the second-order constant.

ground state ($^2\Sigma^+, \nu=0$) after about 1500 ns (200 Torr of N_2O) or 500 ns (>400 Torr of N_2O). (3) Ground-state $\text{AlO}(^2\Sigma^+, \nu=0)$ shows no appreciable reactivity with N_2O at 296 K. As a result, N_2O can act as an oxidant of Al atoms, a vibrational relaxant for vibrationally excited AlO , and a buffer gas for AlO reactions with other molecules. In contrast, ethylene oxide, which exhibits a rate constant for Al atom oxidation at 296 K which is more than an order of magnitude greater than that of the reaction of Al with N_2O , cannot be used for AlO reaction kinetics studies. This is due to the fact that AlO reacts rapidly with ethylene oxide at room temperature.

The usefulness of the $\text{Al} + \text{N}_2\text{O}$ reaction as a source of AlO for reaction kinetics studies depends on the ability to achieve a fully relaxed, ground-state AlO population within a short time ($\sim 1 \mu\text{s}$). The $\text{Al} + \text{N}_2\text{O}$ reaction is highly exothermic ($\sim 81 \text{ kcal mol}^{-1}$), and is known to result in the production of both the $\text{A}^2\Pi$ and $\text{B}^2\Sigma^+$ excited states of AlO .^{10,11} As well, production of the spin-forbidden $^4\Sigma^+$ and $^4\Pi$ states may be energetically feasible,¹⁵ although theoretical work³³ suggests that these are not accessible, and there are no indications from experimental studies of the $\text{Al} + \text{N}_2\text{O}$ reaction^{10–13} that they are produced. Efficient relaxation of these excited states is essential to the present work.

The production of the $\text{A}^2\Pi$ and $\text{B}^2\Sigma^+$ states of AlO in the $\text{Al} + \text{N}_2\text{O}$ reaction has been observed in chemiluminescence where

the $B^2\Sigma^+ \rightarrow X^2\Sigma^+$ transition appears as a structured emission in the 450–550-nm region.^{10,11} Lindsay and Gole¹¹ have concluded that a chemical process leading to the direct population of the $B^2\Sigma^+$ state is the major source of $B^2\Sigma^+ \rightarrow X^2\Sigma^+$ emission in this reaction. Radiative relaxation of the B state of AlO($v=0,1,2$) is known to occur with a lifetime of about 100 ns.¹⁶ Therefore, the lifetime for chemiluminescence observed in the present study (<200 ns) is roughly that of the B state. This observation, as well as the observation of vibrational relaxation in the $X^2\Sigma^+$ ground state after 500 ns at >400 Torr of N_2O pressure, indicates that the major relaxation processes occurring after the initial formation of AlO from Al and N_2O are over after 500 ns. Prolonged relaxation from other excited states of AlO, such as the $A^2\Pi$ state or quartet states of AlO, would be expected to lead to the observation of either prolonged chemiluminescent emission due to radiative relaxation of the A state or steady-state population of the $v=1,2$ levels of the $X^2\Sigma^+$ ground state due to collisional relaxation through the ground-state vibrational manifold. Neither of these occurs to any appreciable extent under the conditions employed in the present study.

The reaction of Al with N_2O is known to yield $A^2\Pi$ AlO as a significant chemiluminescent fraction of the total AlO yield.¹⁰ The $A^2\Pi \rightarrow X^2\Sigma^+$ transitions have much lower band oscillator strengths than the $B^2\Sigma^+ \rightarrow X^2\Sigma^+$ transitions⁷ and therefore the relaxation of the A-state AlO is expected to be much slower than that of the B state in the absence of collisions. This leads one to consider the possibility of a long-lived AlO($A^2\Pi$) population which slowly relaxes to the ground state of AlO within the time range employed in the present study for kinetic analysis. This is unlikely, however, as Gole et al.^{11,12} have shown that extremely efficient collisional transfer occurs between the $A^2\Pi$ and $B^2\Sigma^+$ vibrational manifolds of AlO in the presence of Ar. N_2O is expected to be at least as efficient as Ar in this energy-transfer process, such that at pressures of N_2O in excess of 200 Torr it is likely that $A^2\Pi$ state AlO molecules produced in the Al + N_2O reaction will be rapidly converted to $B^2\Sigma^+$ -state AlO. The latter will undergo rapid radiative relaxation to the ground state, $X^2\Sigma^+$, where relaxation within the ground electronic state vibrational manifold will occur.

Al Atom Oxidation by N_2O and C_2H_4O . The slower rate of reaction of Al atoms with N_2O ($(1.1 \pm 0.1) \times 10^{-11}$ cm³ molecule⁻¹ s⁻¹) compared with C_2H_4O ($(1.3 \pm 0.3) \times 10^{-10}$ cm³ molecule⁻¹ s⁻¹) at 298 K is contrary to that which would be expected on purely thermodynamic grounds, since the O atom bond dissociation energy of N_2O (40 kcal mol⁻¹)⁶ is less than half that of C_2H_4O (84.7 kcal mol⁻¹)³⁴. However, the trend is similar to that observed for oxidation of boron atoms by these same two molecules. Specifically, reaction rates of $(2.1 \pm 0.8) \times 10^{-14}$ cm³ molecule⁻¹ s⁻¹ (N_2O) and $(3.0 \pm 1.2) \times 10^{-11}$ cm³ molecule⁻¹ s⁻¹ (C_2H_4O) have been obtained in flow tube experiments^{35,36} for these boron atom reactions at 300 K. These variations indicate that other factors such as spin and orbital correlation restrictions are important aspects of the overall reaction mechanism. Interestingly, the exothermicities of the reactions of B atoms with C_2H_4O ³⁷ and N_2O ³⁵ are considerably greater than the corresponding Al atom reactions, yet both Al atom reactions proceed at a much faster rate at room temperature. This trend may point to the importance of close-range electron transfer in the reaction mechanism and reflect the lower ionization potential of Al (6.0 eV) relative to that of B (8.3 eV).³⁸

The faster reaction of Al with C_2H_4O compared with N_2O may arise from the formation of a bound collision complex in the case of C_2H_4O but not for N_2O . Such a mechanism has been proposed for the reaction of B atoms with C_2H_4O .^{35,39} The initial formation

of a bound complex which rearranges to products in the case of the Al + C_2H_4O reaction seems likely in view of the observation of stable complexes between Al atoms and several simple ethers, with binding energies in the range 9–12 kcal mol⁻¹.¹ The direct observation of AlO as a reaction product and the observation of a buffer gas pressure-independent reaction rate indicates that O atom transfer is a major product channel in the Al + C_2H_4O reaction.

Complex Formation Reactions of AlO. The reactions of ground-state AlO($^2\Sigma^+, v=0$) examined in the present study indicate that association complex formation reactions involving third-body stabilization of collision complexes of AlO with a variety of molecules are a major aspect of AlO chemistry at room temperature. Association complexes are implicated by pressure dependence of the pseudo-second-order rate constants for the AlO reactions with CO_2 , CO and ethylene and are probably involved in reactions of AlO with C_2H_4O and TME, as discussed below. Complex formation by AlO is similar to that which has been observed for Al atom reactions with alkenes, arenes, and ethers^{1,2} for which association complexes with binding energies of 9–16 kcal mol⁻¹ have been observed.

The reaction of AlO with CO is of considerable interest in connection with the known non-Arrhenius behavior of the reaction of Al atoms with CO_2 ,^{4,40} for which both abstraction and complexation channels are known at room temperature.⁴ The AlO + CO \rightarrow Al + CO_2 reaction is the reverse of the Al + CO_2 abstraction reaction, a process which is endothermic by about 5 kcal mol⁻¹ if an AlO dissociation energy (D°_0) of 121.3 kcal mol⁻¹ is used.¹⁸ A direct evaluation of the fraction of the total rate for removal of AlO by CO leading to Al atom formation was not possible under the present conditions due to the rapid oxidation of Al atoms by the N_2O buffer gas which would follow formation of Al atoms. Therefore, we were only able to directly measure rate constants for formation of AlO-CO, a competing mechanism for loss of AlO. As the Al + N_2O reaction yields visible chemiluminescence from excited-state AlO relaxation, it was anticipated that, if Al atoms were formed in the AlO + CO reaction, enhanced AlO(B \rightarrow X) emission associated with the aluminum-catalyzed oxidation of CO by N_2O would result. We were unable to detect any increase in the yield of chemiluminescent emission with respect to that observed under conditions of Al oxidation by N_2O where no CO was present.

Formation of an AlO-CO₂ complex is evident in the present study of the AlO + CO_2 reaction. A complex between AlO and CO_2 has been previously suggested by Gole et al.⁴¹ from studies in which perturbed AlO(B \rightarrow X) emission was observed following oxidation of an Al-CO₂ complex by O_3 . Fontijn et al.²¹ have suggested that an AlO-CO₂ complex may be important in the AlO + CO_2 reaction, since a slightly negative activation energy was observed in flow reactor kinetics experiments. The rate constant obtained by Fontijn et al.²¹ for this reaction between 500 and 1400 K and 10–40 Torr of Ar, $(0.7\text{--}12) \times 10^{-14}$ cm³ molecule⁻¹ s⁻¹, is much lower than the value obtained here, $(1.0\text{--}2.0) \times 10^{-11}$ cm³ molecule⁻¹ s⁻¹. The difference is undoubtedly due to the increased contribution from the complex-formation channel at the lower temperature (296 K) and higher pressure (200–600 Torr) employed in the present study.

The reaction of AlO with ethylene shows that complex formation between AlO and molecules containing C–C double bonds is also possible. The AlO + C_2H_4 reaction shows a definite dependence of the pseudo-second-order rate constant on buffer gas pressure between 200 and 700 Torr of N_2O , indicating a complex-formation channel. The AlO + TME reaction does not show pressure dependence between 200 and 700 Torr. However, the lack of observed reactivity between AlO and all alkanes and arenes examined here suggests that the reaction of AlO with TME

(34) Benson, S. W. *Thermochemical Kinetics*; Wiley: New York, 1976.

(35) DiGiuseppe, T. G.; Davidovits, P. J. *Chem. Phys.* **1981**, *74*, 3287.

(36) Tabacco, M. B.; Stanton, C. T.; Davidovits, P. J. *Phys. Chem.* **1986**, *90*, 2765.

(37) Estes, R.; Tabacco, M. B.; DiGiuseppe, T. G.; Davidovits, P. *Chem. Phys. Lett.* **1982**, *86*, 491.

(38) *CRC Handbook of Chemistry and Physics*; CRC Press: Boca Raton, FL, 1983.

(39) Hosseini, S. M.; DeHaven, J.; Davidovits, P. *Chem. Phys. Lett.* **1982**, *86*, 495. Bullitt, M. K.; Paladugu, R. R.; DeHaven, J.; Davidovits, P. *J. Phys. Chem.* **1984**, *88*, 4542.

(40) Fontijn, A.; Felder, W. *J. Chem. Phys.* **1977**, *67*, 1561.

(41) McQuaid, M.; Woodward, J. R.; Gole, J. L. *J. Phys. Chem.* **1988**, *92*, 252.

also occurs via a complexation route. The pressure-independent rate constant indicates that the termolecular reaction is in the high-pressure limit above 200 Torr of N₂O. Association reactions between both ethylene and TME have been observed with Al atoms, the former showing a somewhat larger binding energy.² It is therefore reasonable to expect that TME should form an association complex at room temperature with AlO, if such a process is observed for ethylene. The absence of an appreciable reactivity between AlO and C₆H₆ or C₆H₅CH₃ suggests that the binding energy of an association complex between these molecules is too small for it to remain bound at room temperature (≤ 5 kcal mol⁻¹).

The reaction of AlO with C₂H₄O exhibits a rate constant $(2.1 \pm 0.5) \times 10^{-10}$ cm³ molecule⁻¹ s⁻¹ which is close to the gas kinetic value at 296 K and is pressure independent between 200 and 600 Torr of N₂O pressure. Two possible mechanisms may be considered for AlO consumption: (1) direct abstraction of an O atom to form AlO₂ + ethylene ($\Delta H^\circ_{298} = -11.8 \pm 10$ kcal mol⁻¹), or (2) formation of an AlO-C₂H₄O association complex. High cross sections for either of these reactions could result, in part, from the attractive dipole-dipole forces between AlO ($\mu = 4-5$ D^{7,8}) and C₂H₄O ($\mu = 1.88$ D⁴²). The rate constant for a close collision⁴³ between two molecules with permanent dipoles can be estimated by using a simple electrostatic model,²⁵ which leads to a value of $(8-9) \times 10^{-10}$ cm³ molecule⁻¹ s⁻¹ for the reaction of AlO with C₂H₄O. This is sufficiently close to the experimental value to indicate that the activation energy for the AlO + C₂H₄O reaction is negligible. Such a situation would be consistent with a reaction involving formation of an association complex where bonding occurs through interaction of an oxygen lone pair from C₂H₄O to AlO, in a manner which is analogous to that proposed for Al atom complexes with simple ethers¹ and water.^{44,45}

A high cross section for AlO₂ formation via direct abstraction of O from C₂H₄O seems much less reasonable, in light of the extent of electronic rearrangement which would be involved in breaking the three-membered ring. In order to investigate this possibility further, we studied the reaction of AlO with dimethyl ether (DME), for which the formation of an association complex with AlO similar to that suggested for AlO + C₂H₄O could occur, but for which O atom abstraction is a highly endothermic process. The rate constant for the AlO + DME reaction was found to be $\sim 5 \times 10^{-10}$ cm³ molecule⁻¹ s⁻¹, which is essentially gas kinetic. Therefore, we conclude that, as both reactions of AlO with C₂H₄O and DME exhibit gas kinetic rate constants under similar conditions, both proceed via a complex-formation mechanism.

Abstraction Reactions of AlO. All but one of the reactions examined in the present study are exothermic with respect to abstraction of O, H, or halogen atoms.⁴⁶ Several reactions, such as halogen atom transfer reactions involving CCl₄, CF₃Cl, and CF₃Br, are substantially exothermic (>40 kcal mol⁻¹).⁶ Despite this fact, we have found no direct evidence for an abstraction reaction involving AlO in any of the reactions studied here. All of the reactions in which appreciable reactivity is observed are likely to involve formation of an association complex as discussed

above. It therefore appears that substantial barriers ($E_a \geq 5$ kcal mol⁻¹) exist for all abstraction reactions attempted here.

The ability of AlO to act as a C-H bond oxidizing agent via H atom abstraction, such as is believed to be the role of O⁻ in methane dimerization,⁵ does not appear to be significant at room temperature. The possibility exists that the reactions of surface-bound O⁻ and Li⁺O⁻ with CH₄ involve the concomitant participation of more than one surface site, a scenario which is not possible for diatomic AlO.

The lack of an observed abstraction reaction between AlO and N₂O at 296 K is consistent with the overall trend in reactivity of metal oxides with small oxidants when compared with the corresponding metal atom. Each of the gas-phase reactions of AlO with O₂ and SO₂,^{19,20} and BO with O₂²² as well as NaO with O₃ and N₂O²⁴ exhibit room temperature rate constants which are smaller than the respective metal atom oxidation reaction.^{20,24,35,47} All but NaO + O₃ show a difference in reactivity which is greater than an order of magnitude. The greater than 4 orders of magnitude difference between the rate constants found in this study for the Al/AlO reactions with N₂O is similar to the 3 orders of magnitude difference found in the Na/NaO + N₂O reactions.²⁴ One of the most significant differences between each of the diatomic oxide/atom pairs noted above is the lower ionization potential of the atoms: IP(Al) = 5.98 eV, IP(AlO) = 9.5 eV; IP(Na) = 5.1 eV, IP(NaO) = 6.5 eV; IP(B) = 8.3 eV, IP(BO) = 13.2 eV.⁴⁸⁻⁵¹ This suggests that some degree of charge transfer is important in the mechanisms of these oxidation reactions. The reactivity trends noted above also reflect the general tendency for metathesis reactions involving atoms to exhibit *A* factors which are some 2 orders of magnitude greater than similar reactions which do not involve atoms.³⁴ These factors together suggest that N₂O, as well as other oxidants, may be used as effective O atom sources for studies of metal oxide kinetics in the manner employed in the present work.

Conclusion

We have demonstrated that reaction kinetics measurements can be made on a diatomic metal oxide species in the gas phase using multiphoton dissociation of an organometallic precursor molecule coupled with a fast oxidation reaction. Al atoms are formed by MPD of trimethylaluminum. Ground-state AlO($^2\Sigma^+, v=0$) is formed in high yield following Al atom oxidation by N₂O, which also serves as a buffer gas and a vibrational energy relaxant for AlO. AlO is found to exhibit a chemistry predominantly involving association complex formation reactions with electron-pair donor molecules such as CO₂, CO, ethylene, tetramethylethylene, and ethylene oxide. Reactivity is not observed with several O, H, and halogen atom transfer reagents, despite the fact that several of these reactions are highly exothermic. Thus, appreciable barriers to atom abstraction reactions appear to be a general aspect of AlO reactivity.

Registry No. TMA, 75-24-1; AlO, 14457-64-8; C₂H₄O, 75-21-8; CO, 630-08-0; CO₂, 124-38-9; C₂H₄, 74-85-1; C₂(CH₃)₄, 563-79-1; C₆H₆, 71-43-2; C₆H₅CH₃, 108-88-3; N₂O, 10024-97-2; *i*-C₄H₁₀, 75-28-5; CH₄, 74-82-8; H₂, 1333-74-0; CF₃Cl, 75-72-9; CF₃Br, 75-63-8; CCl₄, 56-23-5.

(42) Cunningham, G. L.; Boyd, A. W.; Myers, R. J.; Gwinn, W. D.; Le Van, W. I. *J. Chem. Phys.* **1951**, *19*, 676.

(43) A close collision refers to one in which the centrifugal barrier is surmounted. See: Johnston, H. S. *Gas Phase Reaction Rate Theory*; Ronald Press: New York, 1966; Chapter 8.

(44) Trenary, M.; Schaeffer, H. F. III; Kollman, P. A. *J. Chem. Phys.* **1978**, *68*, 4047.

(45) Kurtz, H. A.; Jordan, K. D. *J. Am. Chem. Soc.* **1980**, *102*, 1177.

(46) AlO + CO₂ → AlO₂ + CO, $\Delta H^\circ_{298} = +31 \pm 10$ kcal mol⁻¹⁶ is the only exception.

(47) Fontijn, A.; Felder, W.; Houghton, J. J. *Chem. Phys. Lett.* **1974**, *27*, 365.

(48) Huber, K. P.; Herzberg, G. *Molecular Spectra and Molecular Structure 4: Constants of Diatomic Molecules*; Van Nostrand Reinhold: Princeton, NJ, 1979.

(49) Moore, C. E. "Atomic Energy Levels"; Circ. No. 467; *Natl. Bur. Stand. (U.S.)* 1971, Vol. 1.

(50) Hildenbrand, D. L.; Murad, E. *J. Chem. Phys.* **1970**, *53*, 3403.

(51) Rosenstock, H. M.; Draxl, K.; Steiner, B. W.; Herron, J. T. *J. Phys. Chem. Ref. Data* **1977**, *6*, Suppl. No. 1.